19B.2 QUANTITATIVE PRECIPITATION ESTIMATION USING SPECIFIC DIFFERENTIAL PROPAGATION PHASE IN TYPHOON SYSTEMS IN TAIWAN

Yadong Wang*[1], Jian Zhang[1,2], Alexander V. Ryzhkov[1], Lin Tang[1], Kenneth W. Howard[1,2]

[1]Cooperative Institute for Mesoscale Meteorological Studies,
University of Oklahoma, Norman, OK, U.S.A.

[2]National Severe Storms Laboratory, Norman, OK, U.S.A.

1. Introduction

Among different precipitation systems, typhoon is one of the worst threats to Taiwan. On average, 3.3 typhoons hit Taiwan every year, causing damages over 520 million US dollars with extremely heavy rainfalls and strong winds (Lai and Wu 2010). Obtaining accurate quantitative precipitation estimation (QPE) for flood warnings and water resource management during typhoon events is one of the most important missions of the Central Weather Bureau (CWB) of Taiwan. To support this mission, real-time data from two C-band dual-polarization radars, deployed by the Taiwan Air Force, were made available to the CWB.

Even though radar based QPEs have been extensively studied for typical stratiform and convective precipitation systems (e.g. Sachidananda and Zrnic 1987; Chandrasekar et al. 1990; Zrnic and Ryzhkov 1995; Ryzhkov et al. 2004), limited efforts have been focused on QPEs in typhoon systems, especially with the specific differential propagation phase (K_{DP}). In the current study, several existing $R(K_{DP})$ relations were examined with selected typhoon cases and were found to result in severe underestimation. Further investigations indicated that the typhoon systems in Taiwan have unique rain drop size distributions (DSD) and drop shape relations (DSR). To obtain an accurate rainfall estimates in these typhoon systems, a new $R(K_{DP})$ relation was developed for the two operational C-band dual-polarization radars in Taiwan.

In addition to the unique DSD and DSR characteristics, the Central Mountain Range (CMR) of Taiwan (Fig.1) poses a major challenge for radar based QPEs. The power related radar variables such as Z and Z_{DR} on the lower tilts are significantly biased by beams blockages caused by the CMR. Even though the K_{DP} was reported as insensitive to beam shielding up to 90% (Friedrich et al. 2007), plenty of missing or unreliable data are often found at low altitudes due to beam shielding. To assure the quality of K_{DP} data for QPEs, unreliable values from blocked areas need to be replaced by good K_{DP} data either from neighboring unblocked areas on the same tilt (if the blocked section is small) or from the upper and unblocked tilts at the same range/azimuth location (if the blocked section is large). When the upper level K_{DP} data is used for QPEs, a potential error could be introduced if a large variation exists in the vertical profile of K_{DP}. To minimize such errors, a vertical profile correction is applied to K_{DP} values from the high altitudes before they are used in QPEs. The proposed $R(K_{DP})$ relation and the vertical K_{DP} correction method are tested on the two C-band dual-polarization radars in Taiwan, and are evaluated using a dense gauge network for two typhoon events occurred during 2009 and 2010.

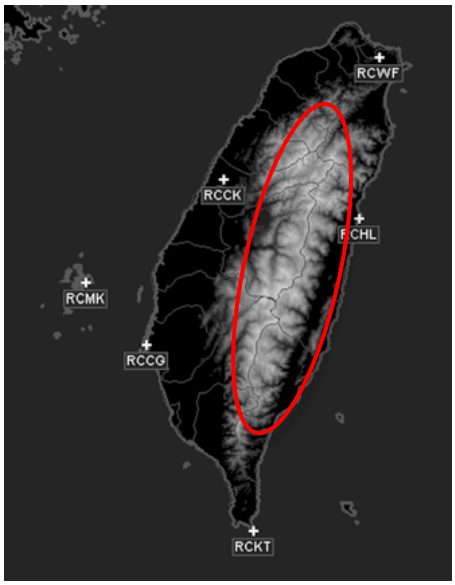

Fig.1. Locations of 4 S-band single-polarimetric radars (RCCG, RCKT, RCHL, RCWF) and 2 C-band dual-polarimetric radars (RCMK, RCCK). The location of central mountain range is depicted by a red circle.

This paper is organized as follows. The new $R(K_{DP})$ rainfall estimation method is introduced in section 2. The vertical profile correction of the specific

*Corresponding author address: Yadong Wang, Cooperative Institute for Mesoscale Meteorological Studies, University of Oklahoma, Norman, Oklahoma 73072; e-mail: Yadong.wang@noaa.gov

differential phase is presented in section 3. Performances of the new methods are examined using two typhoon cases in section 4. Finally, a summary and conclusions are given in section 5.

2. Rainfall Rate Estimation from Specific Differential Phase

DSDs and DSRs play critical roles in the development of radar based QPE algorithms (e.g., Sachidananda and Zrnic 1987; Ryzhkov and Zrnic 1995; Gorgucci et al. 1993, 2001). Parameters such as rainfall rate, liquid water content can be estimated for a pre-determined DSD (e.g., Sachidananda and Zrnic 1987; Ryzhkov and Zrnic 1995; Gorgucci et al. 1993; Zhang et al. 2001). On the other side, the rainfall rate algorithms could vary under different DSR assumptions (Zhang et al. 2001; Teschl et al. 2008). Various combinations of Z, K_{DP} and Z_{DR} have been developed for radar QPEs through numerical simulations and real case measurements (e.g., Brandes et al. 2002; Bringi et al. 2003; Tokay et al. 2008). It was found that the reflectivity based QPE algorithms are more sensitive to DSDs while the polarimetric variable based algorithms are more sensitive to DSRs.

Chang et al. (2009; hereafter CCWL09) found, based on the studies of 13 cases, that the DSD and DSR characteristics of typhoon systems in Taiwan were significantly different from typical maritime or continental precipitation systems. CCWL09 considered these unique characteristics as the features of terrain-influenced convective systems during typhoon landfalls.

The concept of QPE using K_{DP} was firstly introduced by Seliga and Bringi (1978). The relationships between R and K_{DP} for S-band radars were then derived based on simulated and measured DSR (e.g. Sachidananda and Zrnic 1987; Chandrasekar et al. 1990). A modified formula proposed by Ryzhkov and Zrnic (1998a) was suggested to deal with negative K_{DP} values and to further reduce the bias in accumulated rainfalls. The relationships between rainfall rate and K_{DP} for C-band radars were also studied in previous works (e.g. Aydin and Giridhar 1991, Scarchilli et al. 1992). Examples of relations were suggested through simulations by Ryzhko (hereafter Ryzhkov), Scarchilli and Gorgucci (1992), (hereafter SG92), and through a least square fitting based on a large number of measurements by Aydin and Giridhar (1991) (hereafter AG91). Following the approach proposed by Zhang et al. (2001), a new $R(K_{DP})$ relation was derived using the DSD and DSR models proposed by CCWL09 as:

$$R = 35.36K_{DP}^{0.799} \quad (mmh^{-1}) \tag{1}$$

The new and three aforementioned $R(K_{DP})$ relations (Ryzhkov, SG92 and AG91) are listed in Table 1 and plotted in Fig. 2. A fifth $R(K_{DP})$ relation, obtained through a fitting of 12-hour K_{DP} observations with hourly gauge data, is also presented in Fig. 2. The K_{DP} collected by radar RCMK and gauge data used for the fitting were from 0000 UTC to 1200 UTC on 9 August 2009 during typhoon Morakot. In order to eliminate the effect from CMR on the K_{DP} data, only the K_{DP} field within the range of 100 km from RCMK (unblocked region) is used in the fitting procedure. Within this range, 200 gauge stations were used.

Fig. 2 shows significant differences between the three previously reported $R(K_{DP})$ relations and the newly simulated relation from the current study. The difference in R increases with increasing K_{DP}, and the maximum difference is above 50 mm hr^{-1} when K_{DP} is 5^{o}km^{-1}. The simulated $R(K_{DP})$ relation matches the K_{DP}-gauge fitted $R(K_{DP})$ relation very closely, with the maximum difference between the two less than 5 mm hr^{-1}. Therefore, the simulated $R(K_{DP})$ relation is used in the following analysis as the representative of new proposed relation. From the plots, it is evident the three previously reported $R(K_{DP})$ relations could result in large underestimations if used in the QPE for typhoon systems in Taiwan. The new $R(K_{DP})$ relation, on the other hand, appears to be representative of the typhoon precipitation environment and is expected to provide relatively accurate rainfall estimates. The new proposed relation has been applied to independent typhoon events and the results are presented in section 4.

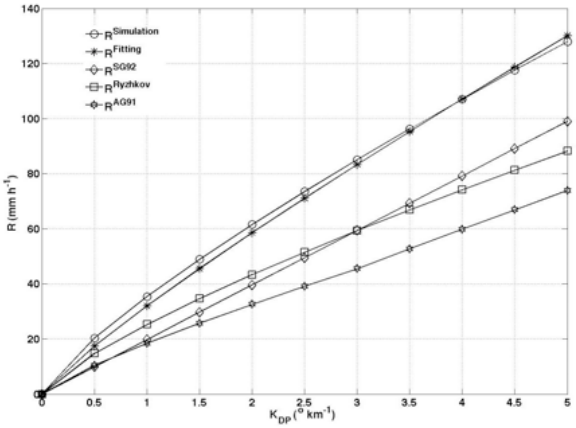

Fig. 2. Comparison of the different $R(K_{DP})$ relationships at C-band. The $R^{simulation}$ and $R^{Fitting}$ indicate the relations derived for typhoon system in Taiwan through simulation and fitting, respectively.

Source	DSD Model	DSR Model	$R(K_{DP})$
Simulation	CCWL09	CCWL09	$R = 35.36K_{DP}^{0.799}$
SG92	Ulbrich83	PB70	$R = 19.8K_{DP}$
Ryzhkov	OK DSD	BZV02	$R = 25.30K_{DP}^{0.776}$
Fitting	Real Case Fitting		$R = 31.97K_{DP}^{0.799}$
AG91	Real Case Fitting		$R = 18.45K_{DP}^{0.82}$ $0.01 < K_{DP} < 3$ $R = 16.03K_{DP}^{0.82}$ $3 \le K_{DP} < 15$

Table 1. $R(K_{DP})$ relations used in this work.

3. Vertical Profiles of Specific Differential Phase

Although K_{DP} was reported immune to partial blockages, missing or questionable data are frequently observed when heavy blockage presents. An example of the K_{DP} fields from RCMK at the two lowest EAs (0.5° and 1.4°) are presented in Fig. 3, where plenty of missing data were observed on 0.5°. If only the K_{DP} from 0.5° is used in QPEs, the rainfall rate field would have a void between 100 to 150 km of range and 80° and 110° of azimuth. Within this region, the K_{DP} values from 1.4° are available that may be used for QPEs in the data void. However, the estimated results are subject to errors induced by vertical variations of K_{DP}. To demonstrate the vertical profile of K_{DP}, a Range Height Indicator (RHI) of K_{DP} observed by RCMK at 0400 UTC 9 August 2009 is shown in Fig. 4, and the height of the melting layer is approximate 5.5 km. At the range of approximate 80 km, K_{DP} values from the lowest file EAs (0.5°, 1.4°, 2.4°, 3.4° and 6°) are around 1.9° km^{-1}, 1.59° km^{-1}, 1.19° km^{-1}, 0.719° km^{-1} and 0.3° km^{-1}, respectively. It appeared that there was a linear decrease in the vertical profile of specific differential phase (VPSDP). Therefore, if the KDP from EA of 1.4° were directly used for the QPE, a 17 mm hr^{-1} underestimation would be resulted in the rain rate according to the new $R(K_{DP})$ relationship (Eq.1). This example indicates that a correction for the non-uniform VPSDP is necessary for accurate dual-pol radar QPEs in areas with significant blockages. Many previous studies on reflectivity-based radar QPEs presented similar findings for the reflectivity field (e.g. Marzano et al. 2004; Andrieu and Creutin 1995). Inspired by the vertical profile of reflectivity (VPR) correction methods, a novel VPSDP correction method is developed in current work.

To understand the vertical distributions of K_{DP}, RCMK observations from 12 hours (0000 UTC 1200 UTC on 9 August 2009) during typhoon Morakot were analyzed. The K_{DP} values from the lowest tilts within range of 100 km ~ 150 km and azimuth of 65° ~ 80°, which are unblocked and close to the mountains, were selected. These K_{DP} were averaged along range of 5 km to mitigate the fluctuation. The averaged K_{DP} values are then normalized against the K_{DP} values from the lowest tilt. The normalized values are plotted in Fig.5 as a function of height Above Radar Level (ARL). The data from the 50 km x 15 deg section over a 12 hours time period showed a clear trend of decreasing K_{DP} with increasing altitude as indicated in Fig. 5.

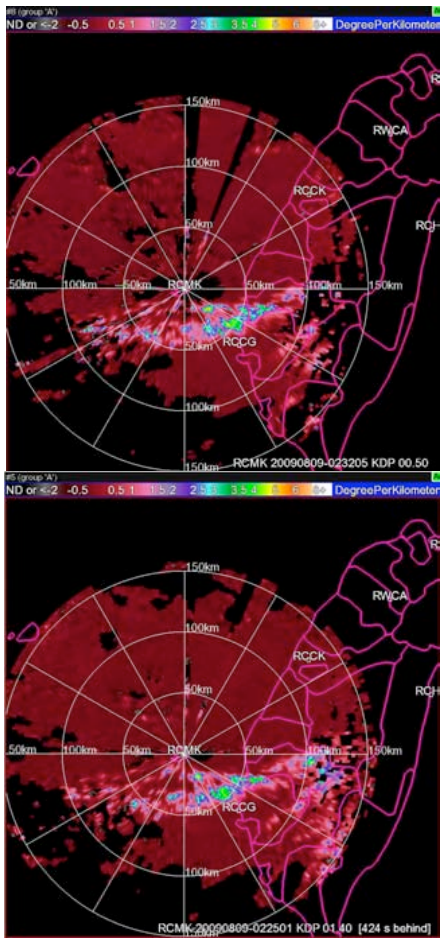

Fig. 3. The PPI of K_{DP} from 0.5 deg. EA (top) and from 1.4 deg. EA (bottom). Severe blockage from 0.5 deg. EA causes plenty of missing data.

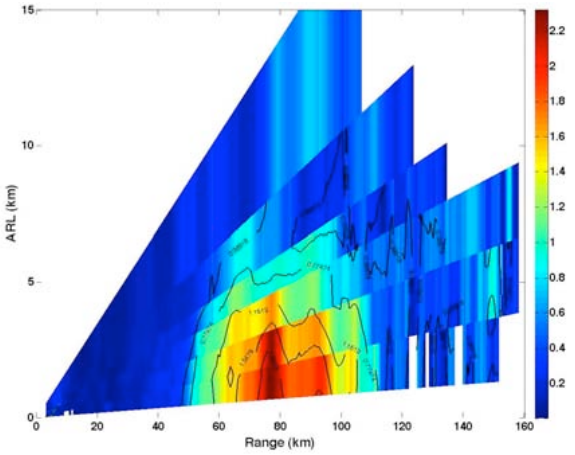

Fig. 4. The range height indicator of K_{DP} field.

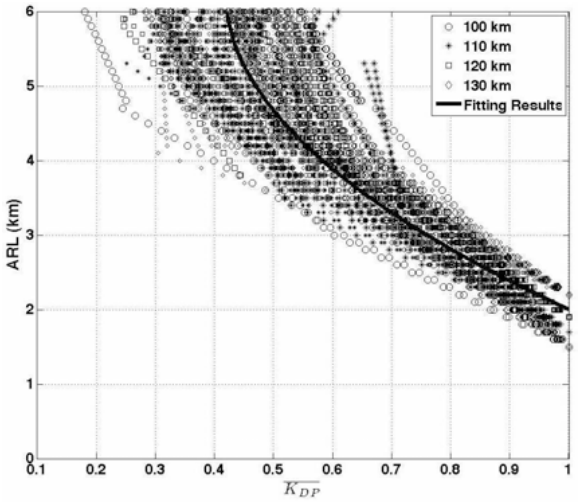

Fig. 5. Scatter plot of the normalized K_{DP} ($\overline{K_{DP}}$) as a function of height of ARL (km). The $\overline{K_{DP}}$ values from different ranges are represented by different symbols. The polynomial fitting results is also inserted with the solid line.

From these data, a VPSDP was generated using a second-order polynomial fitting (bold black line in Fig.5) between the normalized K_{DP}, κ, and the height, h:

$$\kappa(h) = \alpha h^2 + \beta h + \gamma \qquad (2)$$

where h is in km ARL and κ is dimensionless with a value between 0 and 1. The coefficient α, β and γ are determined through the polynomial fitting to the data. The α, β and γ derived in Fig. 5 are 0.032, -0.4009 and 1.6752, respectively. In real-time, the coefficients could be updated every hour based on radar observations. Once the normalized VPSDP is obtained, a vertical correction is applied to the $K_{DP}(h)$ observation via the following equation:

$$K_{DP}^{'}(h_0) = K_{DP}(h)\frac{\overline{K_{DP}(h_0)}}{\overline{K_{DP}(h)}} \qquad (3)$$

where h_0 is the reference height (e.g., at the surface) for the radar QPE, and $K_{DP}^{'}(h_0)$ is the corrected K_{DP} value. Because of the dramatic changes of K_{DP} within the melting layer, this VPSDP correction method is only applied below the melting layer. Further, the VPSDP correction is only applied to pre-defined blockage areas. For each radar and each blocked area, one VPSDP was derived from a neighboring non-blocked region. The VPSDP is assumed to be the same in the non-blocked area and the associated blocked areas, and the VPSDP correction is applied to the K_{DP} observations in the blocked area, which are from the un-blocked but high tilts. The corrected K_{DP} data are then used for the radar QPE. The performance of the VPSDP correction method will be evaluated using real data in section 4.

4. Performance Evaluation

4.1 Experimental description

The new $R(K_{DP})$ relationship and the VPSDP correction method are assessed using two typhoon cases occurred in August 2009 (Morakot) and September 2010 (Fanapi) in Taiwan. Morakot is of a primary interest because of its long duration, record-breaking heavy rain, and because of the tremendous losses of lives and properties that it had caused. After its landfall in Taiwan in the midnight of 8 August 2009, Morakot brought a peak rainfall accumulation of 2874 mm. Over 700 people were reported killed by the storm, and the property loss was more than 3.3 billion US dollars. Fanapi formed on 14 September 2010 and made its first landfall in Taiwan on 19 September. It caused 105 fatalities and approximately 100 million US dollars worth of damages.

Total of three QPE experiments were carried out for the two typhoon events. Among them, two were using different $R(K_{DP})$ relations with the two C-band dual-polarization radars, and one was using a $R(Z)$ relation ($Z = 32.5R^{1.65}$) with the four operational S-band single-polarization radars (i.e., RCWF, RCHL, RCCG, and RCK, Fig.1). For EXPs I – II, the radar QPEs were computed following these five steps:

1) For each individual radar, derive a 2-D "hybrid-scan" K_{DP} field on the polar grid using the lowest and unblocked gates from the volume scan data;
2) Apply a VPSDP correction in the blocked areas

when deemed necessary (e.g., in EXPs II);

3) Compute the rain rate field from the uncorrected (EXP I) or corrected (EXPs II) K_{DP} fields using the designated $R(K_{DP})$ relations In the current study, negative rainfall rates were not allowed and the minimum K_{DP} value used for $R(K_{DP})$ relation was 0^o km^{-1}.
4) Remap the polar grid rain rate fields from single radar onto a common regional Cartesian grid via a nearest neighbor approach. The regional domain covers the area shown in Fig.1 with a spatial resolution of ~1 km x 1 km.
5) Merge the two single radar Cartesian rain rate fields into one regional rain rate field using an inverse-distance weighted mean scheme (Zhang et al. 2008).

For EXP III, the radar QPE was computed based on the following procedure:

1) For each individual S-band radar, derive a 2-D "hybrid-scan" reflectivity (Z) field on the polar grid using the lowest and unblocked gates from the volume scan data;
2) Remap the polar grid Z fields from single radar onto the common regional grid discussed earlier;
3) Mosaic the four single radar Cartesian Z fields into one regional reflectivity mosaic grid using the same inverse-distance weighted mean scheme for the rain rate mosaic;
4) Compute the rain rate field from the mosaiced Z field using the designated $R(Z)$ relation.

Two questions are to be answered through these experiments: 1) is the VPSDP correction more advantages than no-VPSDP correction with respect to the dual-pol radar QPE? and 2) can the C-band dual-polarization radars, with the new $R(K_{DP})$ relation and the VPSDP correction, provide comparable or more accurate QPEs than S-band single-polarization radars? The radar QPEs from each experiment are compared with surface gauge observations and the performances are quantified using the following three statistical scores:

1. Ratio Bias

$$Bias = \overline{R} \Big/ \overline{G} \tag{4a}$$

$$\overline{R} = \frac{1}{N}\sum_{k=1,N} r_k \tag{4b}$$

$$\overline{G} = \frac{1}{N}\sum_{k=1,N} g_k \tag{4c}$$

Here $\overline{R}$ and $\overline{G}$ are the averaged radar and gauge precipitation accumulations, respectively. The r_k and g_k represent a matching pair of the radar-derived and gauge observed rainfall and N represents the total number of matching gauge and radar pixel pairs in the entire spatial and temporal domain. A matching pair of radar-gauge is found if: 1) the gauge location is within the boundary of a 1*km* by 1*km* radar pixel and 2) both the radar estimate r_k and the gauge observation g_k are greater than zero. r_k is an average radar rainfall in 5km by 5km box which is centered at the corresponding gauge. A ratio bias of value greater (less) than 1.0 indicates that the radar has overestimated (underestimated) rainfall assuming accurate gauge reports.

2. Root mean square error (RMSE)

$$RMSE = \left[\frac{1}{N}\sum_{k=1,N}(r_k - g_k)^2\right]^{1/2} \tag{5}$$

3. Correlation Coefficient (CC)

$$CC = \frac{\frac{1}{N}\sum_{k=1,N}\left(r_k - \overline{R}\right)\left(g_k - \overline{G}\right)}{\sigma_r \sigma_g} \tag{6a}$$

$$\sigma_r = \sqrt{\frac{1}{N}\sum_{k=1,N}\left(r_k - \overline{R}\right)^2} \tag{6b}$$

$$\sigma_g = \sqrt{\frac{1}{N}\sum_{k=1,N}\left(g_k - \overline{G}\right)^2} \tag{6c}$$

4.2 Experimental results

The impact of the VPSDP correction was evaluated using 24 hours data from 0000UTC 9 August to 0000UTC 10 August 2009. C-band dual-polarization radar QPEs from EXPs I (no VPSDP correction) and II (with VPSDP correction) are compared with the gauge observations and results are shown in Fig. 6. The simulated relation of $R = 35.36K_{DP}^{0.799}$ is used in the rainfall rate estimation. Since the VPSDP correction method is mainly applied along the CMR (within the region marked by yellow circle), only a portion of the radar coverage associated with 217 gauges is selected in the evaluation. Fig. 6A shows the spatial distribution of the radar QPE bias ratio without the VPSDP correction, in which the size of the circles represents gauge observed 24-hr rainfall amounts and the color of the circles indicates the bias (e.g., white represents a ratio bias value of 1.0 or no bias; orange represents less than 1.0 or underestimation; and blue represents greater than 1.0 or overestimation).

The underestimation was very evident along the CMR, where the 24-hr gauge amounts are mostly above 10 inches and the radar QPE was about 40 – 80% underestimation (dark orange colored circles along the CMR in Fig.6A). The Bias, CC and RMSE scores for the radar QPE without the VPSDP correction are 0.72, 0.61 and 120.70 mm, respectively. The significant underestimation along the CMR was due to the fact that the K_{DP} data from high elevation angles were used in the rain rate calculation without any correction for the vertical variations.

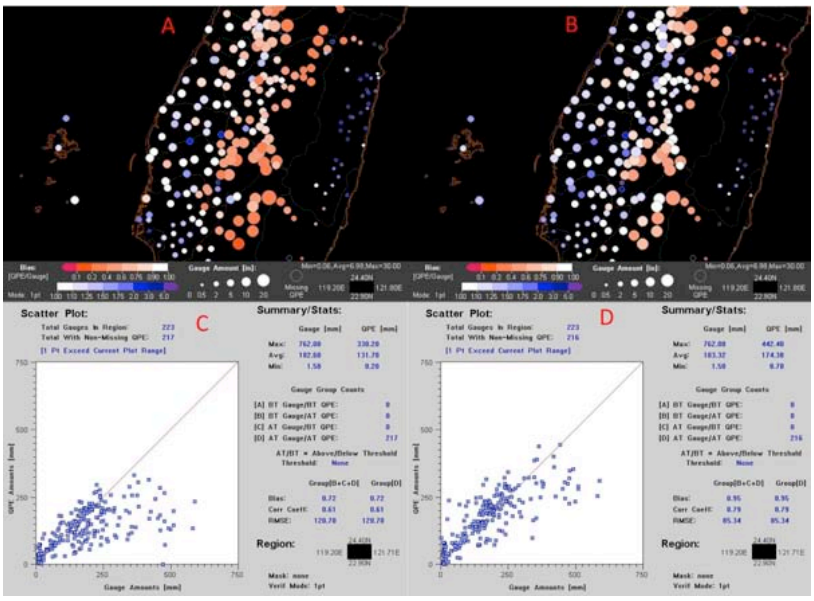

Fig. 6. Comparison of the QPE obtained from before and after VPSDP correction. The bubble charts (A and B) show bias ratios between the QPEs and independent gauge observations, where the size of the circles represents the gauge observed rainfall amount and the color shows the bias. The scatter plots (C and D) shows distribution of the 24 hours QPEs vs. the gauge observations.

Those K_{DP} data did not represent values near the ground and were smaller than the latter based on the VPSDP shown in Fig. 5. After the VPSDP correction was applied, the underestimation was reduced to 0-30% at most of the stations along the CMR (white to light pink colored circles along CMR in Fig. 6B). The improvement was especially significant for heavy rainfall amounts with the 24-hr accumulation higher than 250mm (Fig.6D). All three scores of Bias, CC and RMSE are largely improved after the VPSDP correction (0.95 vs. 0.72 for BIAS, 0.79 vs. 0.61 for CC and 85.34 vs. 120.70 mm for RMSE). These results showed the importance of a VPSDP correction in obtaining accurate dual-polarization radar QPEs using $R(K_{DP})$ relations. The K_{DP} value from higher elevation angle is corrected under the assumption that the vertical profile of K_{DP} from the mount region is similar to the plain region.

The impact of the two C-band dual-polarization radars on operational QPEs for Taiwan was also assessed in the current study. Before the two C-band dual-polarization radars were deployed, the CWB operational radar QPE was produced using four S- band single-polarization radars (Fig.1). In the current study, the S-band radar QPE was calculated using a single $R(Z)$ relation ($Z = 32.5R^{1.65}$), which was used for tropical rainfalls in the operational QPEs for Taiwan (Zhang et al. 2008). Three 24-hr rainfall accumulations (EXP III) were computed for typhoon Morakot and Fanapi events using the S-band radars. The S-band radar QPEs were compared with the C-band dual-polarization radar QPEs (EXP II), and ratio BIAS, CC, and RMSE scores were calculated against gauge observations. The C-band dual-polarization radar QPEs were generated using the new typhoon $R(K_{DP})$ relation and the hourly VPSDP corrections.

The four S-band radars provide relatively good coverage in the north, south, and west parts of Taiwan Island. However, the coverage along the east cost was relatively poor. The steep slope of the CMR near the east coast causes severe blockages immediately to the west of RCHL radar, and poses significant challenges to the operational S-band radar QPEs in the region (Zhang et al. 2008). Therefore, the comparison between the C-band and S-band radar QPEs are restricted to the western 2/3 of the Taiwan Island in the current study.

Fig. 7 shows scatter plots of the 24 hours (0000UTC 9 August to 0000UTC 10 August 2009) radar based QPEs versus the gauge observed 24-hr rainfalls. The quantitive comparison is presented in Table 3. Compared with the 4 S-band QPE, the 2 C-band QPE shows higher CC, lower RMSE and comparable BIAS. It should be noted that the coefficients of Eq. 5 is fitted from hourly. Since 2 C-band dual-polarization radars show better performance than 4 S-band single-polarization

radars, emerge them into the existing radar network can significantly enhance the accuracy of the radar based QPE. Using the similar approach as described in typhoon Morakot, 24 hours QPEs estimated from C-band and S-band radars are applied typhoon Fanapi (0000UTC 19 September to 0000UTC 20 September 2010). The comparison results are also presented in Table 2. Compared to the S-band QPE, slight overestimation on BIAS (1.17 vs. 1.22) can be observed from the C-band radars. However, significant improvement on CC (0.73 vs. 0.86) and RMSE (152.45 vs. 97.55) can be obtained.

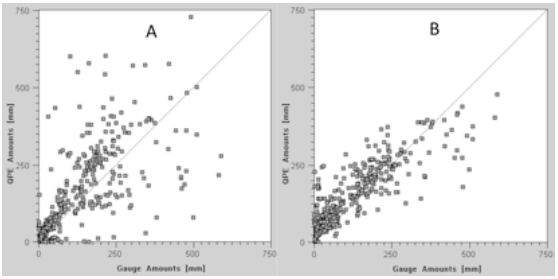

Fig. 7. The scatter plot of the 24 hours QPEs vs. gauge observations on 9 August 2009 from typhoon Morakot. The QPE from 4 S-band radars and 2 C-band radar are on panel A and B, respectively.

9 August 2009			
Algorithm	BIAS	C. C.	RMSE (mm)
2 C-band	0.95	0.85	69.04
4 S-band	1.01	0.65	96.22
19 September 2010			
2 C-band	1.22	0.86	97.55
4 S-band	1.17	0.73	152.45

Table 2. BIAS, C.C. and RMSE from 2 C-band and 4 S-band radars.

5. Summary and Conclusions

To obtain accurate quantitative precipitation estimation for typhoon systems of Taiwan, two new approaches were developed in current work: one is a new $R(K_{DP})$ relation according to the characteristics of DSD and DSR in typhoon systems of Taiwan, and the other is a new vertical profile specific differential phase correction method. Compared to other relations derived based on the DSR for typical maritime or continental precipitation systems, the new relation can provide higher rainfall rate for same K_{DP} value. The new approaches are evaluated with two independent typhoon systems. The 2 C-band dual-polarization radars with the new approaches are shown to provide improved QPEs compared to the 4 S-band single-polarization radars.

References

Andrieu, H. and Creutin, J. D. (1995). Identification of vertical profiles of radar reflectivity for hydrological applications using an inverse method. Part I: formulation. *J. Appl. Meteorol.*, 34:225–239.

Aydin, K. and Giridhar, V. (1991). C-band dual-polarization radar observables in rain. *J. Atmos. Oceanic Technol.,* 9:383–390.

Brandes, E. A., Ryzhkov, A. V., and Zrnic, D. S. (2001). An evaluation of radar rainfall estimates from specific differential phase.

Brandes, E. A., Zhang, G., and Vivekanandan, J. (2002). Experiments in rainfall estimation with a polarimetric radar in a subtropical environment.

Bringi, V. N., V. Chandrasekar, J. H., Gorgucci, E., Randeu, W. L., and Scoenhuber, M. (2003). Raindrop size distribution in different climatic regimes from disdrometer and dual-polarized radar analysis. *J. Atmos. Sci.*, 60:354–365.

Chang, W.-Y., Wang, T.-C. C., and Lin, P.-L. (2009). Characteristics of the raindrop size distribution and drop shape relation in typhoon systems in the western Pacific from the 2D video disdrometer and NCU C-band polarimetric radar. *J. Atmos. Oceanic Technol.*, 26:1973–1993.

Friedrich, K., Germann, U., Gourley, J. J., and Tabary, P. (2007). Effects of radar beam shielding on rainfall estimation for the polarimetric C-band radar. *J. Atmos. Oceanic Technol.*, 24:1839– 1859.

Gorgucci, E., Scarchilli, G., and Chandrasekar, V. (1999). Practical aspects of radar rainfall esti mation using specific differential propagation phase. *J. Appl. Meteorol.*, 39:945–955.

Gorgucci, E., Scarchilli, G., and Chandrasekar, V. (2001). Rainfall estimation from polarimetric radar measurements: Composite algorithms immune to variability in raindrop shape-size relation. *J. Atmos. Oceanic Technol.*, 18:1773–1786.

Lai, L.-H. and Wu, P.-H. (2010). Risk analysis of

rice losses caused by typhoon for Taiwan. *Contemporary Management Research*, 6:141–158.

Maddox, R. A., Zhang, J., Gourley, J. J., and Howard, K. W. (2002). Weather radar coverage over the contiguous United States. *Wea. Forecasting*, 17:927–934.

Marzano, F. S., Vulpiani, G., and Picciotti, E. (2004). Rain field and reflectivity vertical profile reconstruction from C-band radar volumetric data. *IEEE Trans. Geosci. Remote Sens.*, 42:1033– 1046.

Matrosov, S. Y., Clark, K. A., Martner, B. E., and Tokay, A. (2002). Measurements of rainfall with polarimetric X-band radar. *J. Appl. Meteorol.*, 41:941–952.

Park, H., Ryzhkov, A. V., Zrnic, D. S., and Kim, K.-E. (2008). The hydrometeor classification algorithm for the polarimetric WSR-88D: descripition and application to and mcs. *Wea. Forecasting*, 24:730–748.

Pruppacher, H. R. and Beard, K. V. (1970). A wind tunnel investigation of the internal circulation and shape of water drops falling at terminal velocity in air. *J. Atmos. Oceanic Technol.*, 96:247– 256.

Ryzhkov, A. and Zrnic, D. (1995). Comparison of dual-polarization radar estimators of rain. *J. Atmos. Oceanic Technol.*, 12:249–256.

Ryzhkov, A. and Zrnic, D. (1995). Comparison of dual-polarization radar estimators of rain. *J. Atmos. Oceanic Technol.*, 12:249–256.

Ryzhkov, A. and Zrnic, D. (1998a). Beamwidth effects on the differential phase measurements of rain. *J. Atmos. Oceanic Technol.*, 15:624–634.

Ryzhkov, A. and Zrnic, D. (1998b). Discrimination between rain and snow with a polarimetric radar. *J. Appl. Meteorol.*, 37:1228–1240.

Sachidananda, M. and Zrnic, D. S. (1987). Rain rate estimates from differential polarization measurements. *J. Atmos. Oceanic Technol.*, 4:588–598.

Scarchilli, G. and Gorgucci, E. (1992). Rainfall estimation using polarimetric techniques at C-band frequencies. *J. Appl. Meteorol.*, 32:1150–1160.

Seliga, T. A. S. and Bringi, V. N. (1978). Differential reflectivity and differential pahse shift: application in radar meteorology. 13:271–275.

Teschl, F., Randeu, W. L., Schonhuber, M., and Teschl, R. (2008). Simulation of polarimetric radar variables in rain at S-, C-and X-band wavelengths. *Adv. Geophys.*, 16:27–32.

Zhang, G., Viekanandan, J., and Brandes, E. (2001). A method for estimating rain rate and drop size distribution from polarimetric radar measurements. *IEEE Trans. Geosci. Remote Sens.*, 39:830–841.

Zhang, J., K. Howard, P.-L. Chang, P. T.-K. Chiu, C.
R. Chen, C. Langston, W. Xia, B. Kaney, and P.-F.
Lin, 2008: High-Resolution QPE System for Taiwan, *Data Assimilation for Atmospheric, Oceanic, and Hydrologic Applications*. S. K. Park,
L. Xu, Ed(s), Springer-Verlag, 147 - 162.

Zrnic, D. S. and Ryzhkov, A. (1995). Advantages of rain measurements using specific differential phase. *J. Atmos. Oceanic Technol.*, 13:454–464.